

# Temperature and Dose-Rate Effects in Gamma Irradiated Rare-Earth Doped Fibers

B. P. Fox, K. Simmons-Potter  
 University of Arizona, Tucson, AZ 85721-0104

W. J. Thomas, Jr.  
 NASA Goddard Space Flight Center, Greenbelt, MD 20771

D. C. Meister  
 Sandia National Laboratories, Albuquerque, NM 87185

R. P. Bambha and D. A. V. Kliner  
 Sandia National Laboratories, Livermore, CA 94551

## ABSTRACT

Rare-earth-doped fibers, such as  $\text{Er}^{3+}$ - and  $\text{Yb}^{3+}$ -doped aluminosilicates can be advantageous in space-based systems due to their stability, their high-bandwidth transmission properties and their lightweight, small-volume properties. In such environments the effect of ionizing-radiation on the optical transmission of these fibers is of paramount importance. For the present work, gamma-radiation experiments were conducted in which un-pumped  $\text{Yb}^{3+}$  and  $\text{Er}^{3+}$  doped sample fibers were irradiated with a Cobalt-60 source under different dose-rate and temperature conditions. In-situ spectral transmittance data over the near IR was monitored during the irradiations for total doses of up to tens of krad (Si). It was found that there was a dose-rate dependence in which higher rates resulted in more photodarkening. Higher temperatures were not found to significantly affect the rate of photodarkening at the dose rates used.

**Keywords:** Gamma-radiation effects, photodarkening, radiation-induced absorption, dose-rate dependence, dose-rate effects, temperature effects, Co-60 irradiation, rare-earth doped fibers

## 1. INTRODUCTION

Fibers doped with rare-earth ions such as erbium 3+ ( $\text{Er}^{3+}$ ) and ytterbium 3+ ( $\text{Yb}^{3+}$ ) allow for the design of rugged, monolithic optical systems with a high bandwidth, excellent beam quality, and the possibility for high-power applications<sup>1-6</sup>.  $\text{Er}^{3+}$ -doped fibers are the most important fiber amplifier in telecommunication due to the ability to amplify signals at the minimum silica absorption wavelength of 1.5  $\mu\text{m}$ <sup>6-8</sup>. Fiber amplifiers doped with  $\text{Yb}^{3+}$ , which can amplify signals near 1.06  $\mu\text{m}$ , experience reduced effects of concentration quenching due to ion-ion interactions, have a low probability for excited state absorption, and can reach a higher electrical-to-optical conversion efficiency than  $\text{Er}^{3+}$ -doped amplifiers<sup>9,10</sup>. High reliability and small volume make these fibers desirable for applications situated in ionizing-radiation environments, and their low weight provides additional incentive for the development of these fibers for space-based systems<sup>11-12</sup>.

It is well known that radiation in low-Earth orbit (LEO) arises from a number of sources including solar events, cosmic rays, and particles trapped in the Van Allen belts<sup>13,14</sup>. For optical materials the radiation sources of primary concern are high energy particles and gamma rays, as these can lead to the formation of color centers (or absorbing centers) in the materials<sup>15-20</sup> which negatively impact fiber performance<sup>21-40</sup>. Determination of the radiation response of these rare-earth-doped fibers, therefore, is central to the design of optical systems for use in harsh radiation environments, as these fibers are often the most radiation-sensitive part of an amplifier system<sup>11,29</sup>. The decrease in

optical transmittance of doped fibers with respect to ionizing-radiation dose and dose rate has been described by a power law<sup>16-20</sup>. Factors affecting the radiation-induced loss observed in doped fibers include the exact type of ionizing radiation, methods of fiber fabrication, total absorbed dose, rare-earth dopant and co-dopant concentrations, as well as temperature and dose rate<sup>8,23,26,30,33,36,40-42</sup>.

Experiments were conducted to provide insight into the effect of elevated temperatures and varying dose-rates on the rate of photodarkening. Spectra over the near-infrared (1.0  $\mu\text{m}$  to 1.6  $\mu\text{m}$ ) were recorded for fibers doped with  $\text{Er}^{3+}$  and  $\text{Yb}^{3+}$  for different irradiation times from a  $\text{Co}^{60}$  source leading to total accumulated doses up to tens of krad (Si). All tests were passive as no pumping of the fibers took place.

## 2. EXPERIMENT

Presented within this paper are the results of experiments in which  $\text{Er}^{3+}$ - and  $\text{Yb}^{3+}$ -doped aluminosilicate fibers from Liekki were exposed to gamma radiation from a  $\text{Co}^{60}$  source in a test cell of the Gamma Irradiation Facility (GIF) at Sandia National Laboratories in Albuquerque, NM. One  $\text{Er}16-8/125$  type  $\text{Er}^{3+}$ -doped fiber was investigated, where the first number designates the nominal peak absorption at 1530 nm in the core in dB/m, and the second and third numbers denote the core and cladding diameters respectively in  $\mu\text{m}$ . In addition, one  $\text{Yb}^{3+}$ -doped fiber was tested with the designation  $\text{Yb}1200-4/125$ , with similar naming convention, except with the peak absorption specified at 976 nm. All fibers were fitted with SMA connectors (Coastal Connections) to facilitate connections to other fibers and test equipment.

Dose-rate and temperature effects on the gamma-radiation-induced photodarkening were investigated using the experimental setup shown in Figure 1. The individual array elements making up the  $\text{Co}^{60}$  source were arranged on a platform, which was raised out of a pool of water into the cell during testing. For the experiments examining dose-rate dependencies, the rare-earth-doped test fibers were spooled and mounted vertically facing the source, to provide uniform irradiation. The individual test fibers were placed at different distances from the source to provide different dose rates ranging from 8.9 rad(Si)/s to 33.4 rad(Si)/s. Data from four  $\text{CaF}_2$  thermoluminescent devices (TLDs) on each spool were averaged to give an indication of the total accumulated dose as well as the dose rate received by each fiber at the various experiment locations within the test cell, while thermocouples were used to monitor sample temperatures throughout the experiment.

Outside of the test cell, broadband reference light from a 75 W xenon arc lamp (Oriel Model 6263) was coupled into a set of delivery fibers by means of collimating optics. The delivery fibers, which carried the optical signal into and out of the test chamber, were SMA connectorized and were standard low-OH silica fibers (Ocean Optics P100-10-VIS/NIR) with a relatively flat transmission spectrum in the near infrared. Special radiation-hard fibers could not be used due to higher OH levels, which introduced unwanted absorption in the wavelength region of interest. Half of the delivery fibers were connected to the ends of spooled, doped test fibers within the test cell. Light coupled into these delivery fibers traveled into the test cell, through the spooled rare-earth-doped test fibers, and then back out of the test cell via the set of return delivery fibers to the diagnostic equipment. These fiber lines constituted the test channels. The other half of the delivery fibers ran in pairs alongside the test-fiber lines, but the input and output fiber pairs were directly connected to one another inside the test cell (i.e.: the segment of doped, test fiber was absent from the fiber line), constituting background channels. Data collected from the background channels in this way was used to evaluate any changes in the transmission signals of the test-fiber lines attributable to losses incurred in the delivery fibers themselves (rather than in the spools of doped fiber). A time-dependent comparison of the spectral signal data with the spectral background data allowed for a direct analysis of gamma-induced losses in the rare-earth-doped fibers under test with the background removed. Data from multiple fiber lines were collected by sampling the fiber outputs sequentially using 1:9 fiber switches (Piezosystems Jena). Transmission spectra were collected on each fiber approximately once per minute, and the effect of radiation-induced optical photodarkening was monitored over a 10 – 20 min period by recording the temporal decrease in the transmittance of the xenon reference light over a broad wavelength window ( $\sim 1.0 \mu\text{m}$  to  $\sim 1.6 \mu\text{m}$ ) using an optical spectrometer (Ocean Optics NIR 512). In addition, as the fiber samples varied in length, all transmission data were normalized to a standardized 1.0 meter fiber length using a standard Beer's law formalization.

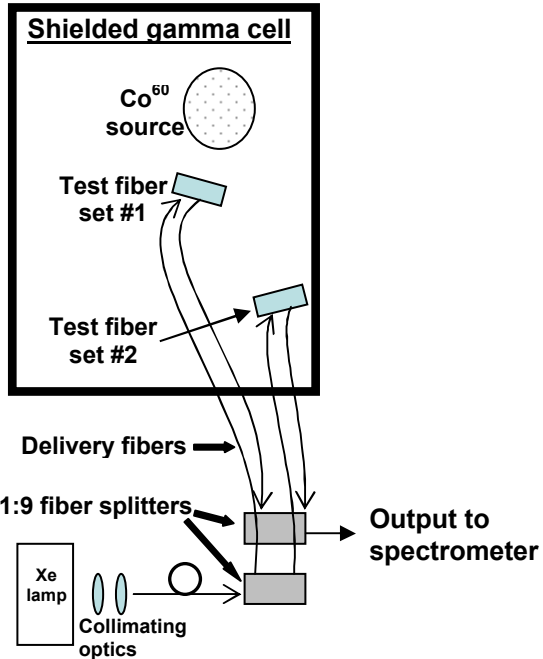


Figure 1: Experimental configuration for test fibers located in gamma test chamber (GIF-A) at Sandia National Laboratories, NM, for radiation exposure studies. Broadband optical radiation from a xenon arc lamp, located outside the test chamber, was coupled into a set of standard  $\text{SiO}_2$  delivery (background) fibers. Delivery fibers entered the test chamber through access ports and coupled light into the test fibers located inside the gamma test chamber. The transmission spectrum over the wavelength range of 1000 nm to 1600 nm, was monitored at 1 min. intervals throughout the gamma exposure for each test and/or background fiber. An Ocean Optic NIR 512 spectrometer was used to monitor spectral data.

The experiments investigating the effect of temperature were conducted similarly to the experiments investigating the dose-rate dependencies as described above, except that the test fiber samples were coiled into milled grooves in aluminum blocks and held in place with a glass cover plate. For these studies, the distances from the fiber mounts to the radiation source was kept constant to deliver dose-rates on the order of 32.5 rad(Si)/s. As in the dose-rate experiments, the fibers in their respective blocks were mounted vertically to assure uniform irradiation. The blocks were heated by cartridge heaters connected to a controller located outside of the test cell and the temperature for the controller was monitored via thermocouples. Elevated temperatures of 50°C, 75°C, and 100°C were used in the testing. Samples were heated and their temperatures were allowed to stabilize prior to the gamma irradiations and sample temperatures were monitored throughout the experiments. Typical temperature variations of less than 2°C were observed during the tests. In addition to the dose-rate and temperature experiments described, samples of the  $\text{Er}^{3+}$ - and  $\text{Yb}^{3+}$ -doped fibers were heated to a temperature of 100°C at dose-rates of approximately 16.5 rad(Si)/s to give information on the combined effects of temperature and dose-rate variations. Results for the experiments are summarized below.

### 3. RESULTS AND DISCUSSION

The various rare-earth-doped sample spectra collected at different irradiation times were normalized to the pre-irradiation spectrum, and then divided by the corresponding normalized spectra of the background channel to obtain a useful representation of the data. Figure 2 shows examples of the processed data from an Er16-8/125 and a Yb1200-4/125 fiber. The figure displays fiber transmittances over the near-infrared, with Figure 2 (a) showing the characteristic absorption at 1.5  $\mu\text{m}$  for  $\text{Er}^{3+}$ -doped fibers, and Figure 2 (b) showing the comparatively flat transmittance spectrum expected for a  $\text{Yb}^{3+}$ -doped fiber. Decreases in the optical transmittance due to gamma-induced color-center absorption can clearly be seen in both plots. These decreases in transmittance become more pronounced as the total accumulated radiation dose increases. At a total accumulated radiation dose of under 20 krad(Si) the transmittance of the  $\text{Er}^{3+}$ -doped

fiber has decayed over 50% across the spectrum shown, while the  $\text{Yb}^{3+}$ -doped fiber only incurs comparable losses at doses over 40 krad(Si), affirming that the  $\text{Er}^{3+}$ -doped fiber is more radiation-sensitive than the  $\text{Yb}^{3+}$ -doped fiber<sup>21</sup>.

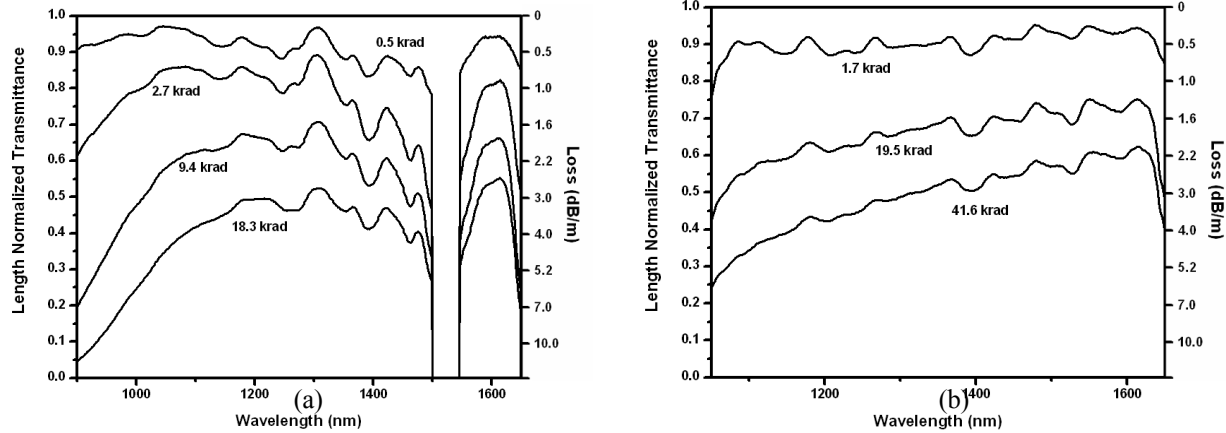


Figure 2: Gamma-radiation-induced decreases in optical transmittance of rare-earth doped fibers. Data are taken from processed spectrometer data of an (a) Er16-8/125 fiber at a dose rate of 30.4 rad(Si)/s and (b) of a Yb1200-4/125 fiber at a dose rate of 32.2 rad(Si)/s.

The Er16-8/125 type fiber was examined for dose-rate dependence at room temperature. Figure 3 shows three of the aforementioned  $\text{Er}^{3+}$ -doped fibers plotted at fixed total accumulated radiation doses under different dose rate conditions. As previously reported, a general trend is observed in which higher dose-rates lead to more photodarkening than the lower dose rates<sup>21,22</sup>. It should be noted that certain regions of the spectrum, e.g. below 1100 nm and the peak just below 1300 nm, experience only little dose-rate dependence, while other regions show a much higher dependence on dose-rate, as for example the region from 1400 nm to just below 1500 nm.

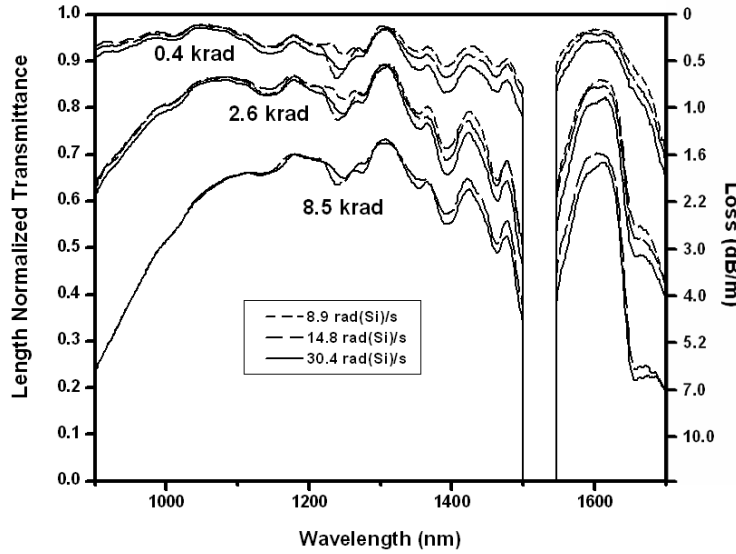


Figure 3: Gamma-radiation-induced decreases in optical transmittance for an Er16-8/125 fiber at different total accumulated doses and dose rates at room temperature.

Examining the behavior of photodarkening at a constant dose-rate over various total accumulated doses at different temperatures gives insight into the temperature dependence of the radiation-induced loss. Figure 4 shows samples of the (a) Er16-8/125 and the (b) Yb1200-4/125 type rare-earth-doped fibers irradiated at the temperatures 50°C, 75°C, and 100°C. For the Er16-8/125 fiber a room temperature curve was also included. Of the wavelengths that were investigated the most reliable trends were found in the low noise regions, which were situated below 1100 nm for the  $\text{Er}^{3+}$ -doped fibers and primarily encompassed the region between 1100 nm and 1300 nm for the  $\text{Yb}^{3+}$ -doped fibers. At the total accumulated radiation doses used, the temperature was not found to significantly affect the photodarkening, but trends could be observed in some of the fibers, the Er16-8/125 fiber showing the strongest trend, with higher temperatures led to increased rates of photodarkening. A similar trend is also observed in the  $\text{Yb}^{3+}$ -doped samples, but the differences in optical transmittances between the samples exposed to the three temperatures was not found to be as large as in the aforementioned  $\text{Er}^{3+}$ -doped fiber.

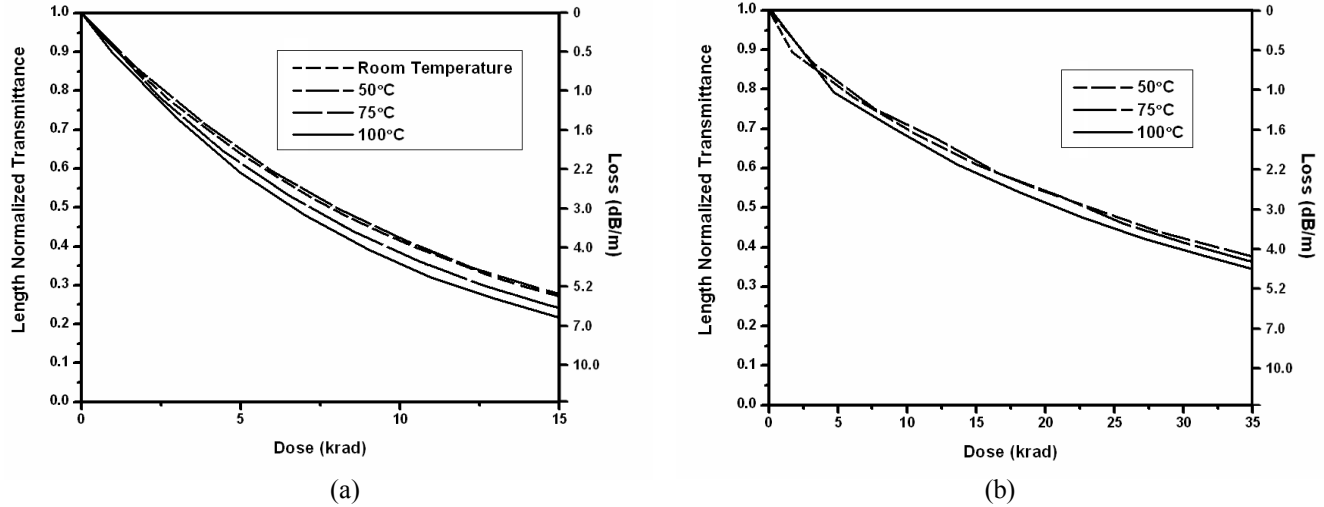


Figure 4: Effect of temperature on photodarkening behavior of gamma-irradiated (a) Er16-8/125, and (b) Yb1200-4/125. Graph for the  $\text{Er}^{3+}$ -doped fiber (a) is for the wavelength 981 nm, while the  $\text{Yb}^{3+}$ -doped fiber (b) is shown for 1100 nm. All samples were exposed at dose rates close to 32.5 rad(Si)/s.

The combined effect of temperature and dose-rate on gamma-radiation-induced photodarkening was investigated in further experiments. The results are plotted in Figure 5 and show that at the elevated temperature of 100°C the Er16-8/125 fiber in (a) still exhibits a weak dependence in which the higher dose-rate leads to increased photodarkening, while the Yb1200-4/125 fiber in (b) shows a reverse dose-rate dependence and exhibits increased photodarkening at lower dose-rates. For the latter type of fiber these effects are seen across the spectrum from below 1100 nm up to 1700 nm. The fibers thus clearly exhibit two distinct dose-rate dependencies that affect the rate of gamma-radiation-induced photodarkening. At low temperatures, a direct positive correlation was observed in all samples between increasing photodarkening rate and increasing dose-rate of exposure. By contrast, at elevated temperatures of 100°C  $\text{Er}^{3+}$ -doped samples exhibited this trend while the  $\text{Yb}^{3+}$ -doped samples showed a decrease in photodarkening rate with increasing dose-rate of exposure. Similar effects have been seen in pure silica fibers<sup>43</sup> and are attributed to the propensity for color-center annealing at elevated temperatures in certain composition types.

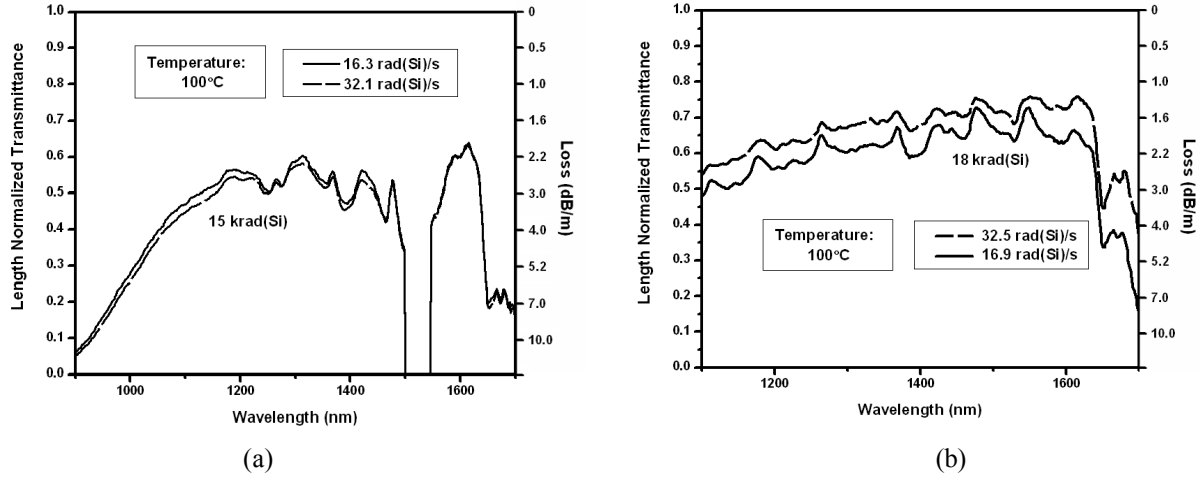


Figure 5: The effect of dose rate on the photodarkening behavior of (a) Er16-8/125, and (b) Yb1200-4/125 rare-earth doped fiber.

#### 4. CONCLUSION

The dose-rate and temperature dependence on gamma-radiation-induced photodarkening was investigated to give insight into the performance of rare-earth-doped optical fibers in ionizing radiation environments such as space. One type of  $\text{Er}^{3+}$ -doped fiber (Er16-8/125) and one type of  $\text{Yb}^{3+}$ -doped fiber (Yb1200-4/125) from Liekki were irradiated with a  $\text{Co}^{60}$  source. The fibers were exposed to the gamma radiation under different dose-rates and at elevated temperature conditions. It was found that the all of the samples tested experienced significant losses due to photodarkening in the near-infrared wavelength region tested. At room temperature, higher dose-rates were found to increase the rate of photodarkening in comparison to lower dose-rates, in agreement with results obtained in previous experiments<sup>21,22</sup>. The elevated temperature data did not show strong dependencies at most wavelengths, but in the low noise spectral regions some trends could be observed. The Er16-8/125 and the Yb1200-4/125 fibers both showed a temperature dependence in which the higher temperatures led to more photodarkening than the lower temperatures (for a given, fixed dose rate), with the effect being more pronounced in the latter materials.

The experiments conducted at an elevated temperature of 100°C and varying dose-rates showed that the Er16-8/125 fiber maintained its dose-rate dependence in which larger dose-rates lead to more photodarkening than lower dose-rates, while the Yb1200-4/125 exhibited the reverse dose-rate dependence resulting in lower dose-rates inducing greater losses than higher dose-rates. This effect highlights the importance the interaction between temperature and dose-rate and shows that the particular dose-rate dependence, i.e. higher or lower rates of photodarkening given a high or low dose-rate, is affected by the absolute dose-rate, the temperature, as well as the fiber composition. It is thus clear that the design of any rare-earth-doped fiber-based optical system operating in ionizing-radiation environments, such as space, requires that the aforementioned factors be taken into account when estimating the effect of photodarkening on the system.

#### 5. ACKNOWLEDGEMENTS

This work was supported jointly by the University of Arizona and the State of Arizona TRIF funds and by Laboratory Directed Research and Development, Sandia National Laboratories, under contract DE-AC04-94AL85000.

## 6. REFERENCES

1. Farrow, R. L., Kliner, D. A. V., Schrader, P., Hoops, A. A., Moore, S. W., Hadley, G. R., and Schmitt, R. L., "High-Peak-Power (>1.2 MW) Pulsed Fiber Amplifier," Proc. SPIE 6102, 61020L (2006).
2. Sumimura, K., Yoshida, H., Fujita, H., and Nakatsuka, M., "Yb Fiber Mode-Locked Laser with a Wide Tuning Range for Chirped Pulse Amplification System," IEICE Electronics Express 3 (11), 233-237 (2006).
3. Jeong, Y., Sahu, J. K., Payne, D. N., and Nilsson, J., "Ytterbium-Doped Large-Core Fiber Laser with 1.36 kW Continuous Wave Output Power," Opt. Exp. 12 (25), 6088-6092 (2004).
4. Brooks, C. D., and Di Teodoro, F., "1-mJ Energy, 1-MW Peak-Power, 10-W Average-Power, Spectrally Narrow, Diffraction-Limited Pulses From a Photonic-Crystal Fiber Amplifier," Opt. Exp. 13 (22), 8999-9002 (2005).
5. Laroche, M., Gilles, H., Girard, S., Passilly, N., and A?t-Ameur, K., "Nanosecond Pulse Generation in a Passively Q-Switched Yb-Doped Fiber Laser by Cr4+:YAG Saturable Absorber," IEEE Photonics Technology Letters 18 (6), 764-766 (2006).
6. Zyskind, J. L., "Erbium-Doped Fiber Amplifiers," Proc. SPIE 158, 14-23 (1991).
7. Miniscalco, W. J., "Erbium-Doped Glasses for Fiber Amplifiers at 1500 nm," J. Lightwave Technology 9 (2), 234-250 (1991).
8. Williams, G. M., Putnam, M. A., Askins, C. G., Gingerich, M. E., and Friebel, E. J., "Radiation Effects in Erbium-Doped Optical Fibres," Electron. Lett. 28 (19), 1816-1818 (1992).
9. Paschotta, R., Nilsson, J., Tropper, A. C., and Hanna, D. C., "Ytterbium-Doped Fiber Amplifiers," IEEE J. Quantum Electron. 33 (7), 1049-1056 (1997).
10. Pask, H. M., Carman, R. J., Hanna, D. C., Tropper, A. C., Mackechnie, C. J., Barber, P. R., and Dawes, J. M., "Ytterbium-Doped Silica Fiber Lasers: Versatile Sources for the 1-1.2  $\mu$ m Region," IEEE Journal of Selected Topics in Quantum Electronics 1 (1), 2-13 (1995).
11. Bussjager, R. J., Hayduk, M. J., Johns, S. T., and Taylor, E. W., "Comparison of Radiation-Induced Passive and Dynamic Responses in Two Erbium-Doped Fiber Lasers," IEEE Aerospace Conf. Proc. 3, 1369-1379 (2002).
12. Caussanel, M., Gilard, O., Sotom, M., Signoret, P., and Gasiot, J., "Extrapolation of Radiation-Induced EDFA Gain Degradation at Space Dose Rate," Electron. Lett. 41 (4), 168-170 (2005).
13. Benton, E. R., and Benton, E. V., "Space Radiation Dosimetry in Low-Earth Orbit and Beyond," Nuclear Instruments and Methods in Physics Research B 184 (1-2), 255-294 (2001).
14. Haskins, P. S., McKisson, J. E., Weisenberger, A. G., Ely, D. W., Ballard, T. A., Dyer, C. S., Truscott, P. R., Piercy, R. B., and Ramayya, A. V., "Gamma-ray measurements from the space shuttle during a solar flare," Adv. Space Res. 12 (2-3), 331-334 (1992).
15. Glebov, L. B., "Linear and Nonlinear Photoionization of Silicate Glasses", Glass Science and Technology 75, C2 (2002).
16. Griscom, D. L., "Nature of Defects and Defect Generation in Optical Glasses," Proc. Soc. Photo-Opt. Instrum. Eng. 541, (1985).
17. Liu, D. T. H., and Johnston, A. R., "Theory of Radiation-Induced Absorption in Optical Fibers," Opt. Lett. 19, 548-550 (1994).
18. Griscom, D. L., Gingerich, M. E., and Friebel, E. J., "Model for the Dose, Dose-Rate and Temperature Dependence of Radiation-Induced Loss in Optical Fibers," IEEE Trans. Nucl. Sci 41 (3), 523-527 (1994).
19. Williams, G. M., Wright, B. M., Mack, W. D., and Friebel, E. J., "Projecting the Performance of Erbium-Doped Fiber Devices in a Space Radiation Environment," Proc. SPIE 3848, 271-280 (1999).
20. Berné, O., Caussanel, M., and Gilard, O., "A Model for the Prediction of EDFA Gain in a Space Radiation Environment," Photonics Technology Letters, IEEE, 16 (10), 2227-2229 (2004).
21. Fox, B. P., Schneider, Z. V., Simmons-Potter, K., Thomes, W. J., Meister, D. C., Bambha, R. P., Kliner, D. A. V., and Söderlund, M. J., "Gamma Radiation Effects in Yb-Doped Optical Fiber," Proc. SPIE 6453, (2007).
22. Fox, B. P., Schneider, Z. V., Simmons-Potter, K., Thomes, W. J., Meister, D. C., Bambha, R. P., and Kliner, D. A. V., "Spectrally-Resolved Transmission Loss in Gamma Irradiated Yb-Doped Optical Fibers," IEEE J. of Quantum. Electron. 44 (6), 581-586 (2008).
23. Lewis, R. B. J., Sikora, E. S. R., Wright, J. V., West, R. H., and Dowling, S., "Investigation of Effects of Gamma Radiation on Erbium-Doped Fibre Amplifiers," Electron. Lett. 28 (17), 1589-1591 (1992).
24. Broer, M. M., Krol, D. M., and DiGiovanni, D. J., "Highly Nonlinear Near-Resonant Photodarkening in a Thulium-Doped Aluminosilicate Glass Fiber," Opt. Lett. 18 (10), 799 (1993).

25. Fukuda, C., Chigusa, Y., Kashiwada, T., Onishi, M., Kanamori, H., and Okamoto, S., “ $\gamma$ -Ray Irradiation Durability of Erbium-Doped Fibres,” *Electron. Lett.* 30 (16), 1342-1344 (1994).
26. McFadden, J. D. O., Greenwell, R., Hatch, J., Barnes, C., Pentrack, D., and Scott, D., “Measurements and Results of Gamma Radiation Induced Attenuation at 980 nm of Single Mode Fiber,” *Proc. SPIE*, 2811, 77-86 (1996).
27. Williams, G. M., Putnam, M. A., and Friebele, E. J., “Space Radiation Effects on Erbium Doped Fibers,” *Proc. SPIE* 2811, 30-37 (1996).
28. Taylor, E. W., McKinney, S. J., Sanchez, A. D., Winter, J. E., Craig, D. M., Paxton, A. H., Ewart, R., Miller, K., O’Connor, T., and Kaliski, R., “Gamma-Ray Induced Effects in Erbium-Doped Fiber Optic Amplifiers,” *Proc. SPIE*, 3440, 16-23 (1998).
29. Bussjager, R. J., Hayduk, M. J., et al., “Gamma-Ray Induced Responses in an Erbium Doped Fiber Laser,” *Aerospace Conference, 2001, IEEE Proceedings 3*, 1473-1479 (2001).
30. Brichard, B., Fernandez, A. F., Ooms, H., Van Uffelen, M., and Berghmans, F., “Study of the Radiation-Induced Optical Sensitivity of Erbium and Aluminum-Doped Fibres,” *Proceedings of the 7th European Conference on Radiation and its Effects on Components and Systems, RADECS 2003, IEEE*, (2003).
31. Johns, S. T., Hayduk, M. J., Bussjager, R. J., Gerhardstein, C. M., Vettese, E. K., Fanto, M. L., and Taylor, E. W., “Temporal Responses of Actively Mode-Locked Erbium-Doped Fiber Lasers Irradiated by Gamma-Rays,” *Electron. Lett.* 39 (18), 1310-1312 (2003).
32. Van Uffelen, M., Girard, S., et al., “Gamma Radiation Effects in Er-Doped Silica Fibers,” *IEEE Trans. Nucl. Sci.* 51 (5), 2763-2769 (2004).
33. Ott, M. N., “Radiation Effects Expected for Fiber Laser/Amplifier Rare Earth Doped Optical Fiber,” *Sigma Research and Engineering / NASA GSFC, Parts, Packaging and Assembly Technologies Office Survey Report*, (2004).
34. Rose, T. S., Gunn, D., and Valley, G. C., “Gamma and Proton Radiation Effects in Erbium-Doped Fiber Amplifiers: Active and Passive Measurements,” *J. Lightwave Technology* 19 (12), 1918-1923 (2001).
35. Koponen, J. J., Söderlund, M. J., and Tammela, S. K., “Photodarkening in Yb-Doped Silica Fibers,” *H. Po Liekki Oy - Proc. SPIE* 5990, 599008 (2005).
36. Taylor, E. W., and Liu, J., “Ytterbium-Doped Fiber Laser Behavior in Gamma-Ray Environment,” *Proc. SPIE* 5897, 58970E (2005).
37. Koponen, J. J., Söderlund, M. J., Hoffman, H. J., and Tammela, S. K. T., “Measuring Photodarkening from Single-Mode Ytterbium Doped Silica Fibers,” *Opt. Exp.* 14 (24), 11539-11544 (2006).
38. Koponen, J. J., Söderlund, M. J., Hoffman, H. J., Kliner, D. A. V., and Koplow, J., “Photodarkening Measurements in Large-Mode-Area Fibers,” *Proc. SPIE* 6453, 64531E (2007).
39. Manek-Hönninger, I., Boullet, J., Cardinal, T., Guillen, F., Ermeneux, S., Podgorski, M., Bello Doua, R., and Salin, F., “Photodarkening and Photobleaching of an Ytterbium-Doped Silica Double-Clad LMA Fiber,” *Opt. Exp.* 15 (4), 1606-1611 (2007).
40. Henschel, H., Köhn, O., Schmidt, H. U., Kirchhof, J., and Unger, S., “Radiation-Induced Loss in Rare Earth Doped Silica Fibres,” *IEEE Trans. Nucl. Sci.* 45 (3), 1552-1557 (1998).
41. Unger, S., Schwuchow, A., Jetschke, S., Reichel, V., Scheffen, A., and Kirchhof, J., “Optical Properties of Yb-Doped Laser Fibers in Dependence on Codopants and Preparation Conditions,” *Proc. SPIE* 6890 ,689016 (2008).
42. Girard, S., Tortech, B., Régnier, E., Van Uffelen, M., Gusarov, A., Ouerdane, Y., Baggio, J., Paillet, P., Ferlet-Cavrois, V., Boukenter, A., Meunier, J.-P., Berghmans, F., Schwank, J. R., Shaneyfelt, M. R., Felix, J. A., Blackmore, E. W., and Thienpont, H., “Proton- and Gamma-Induced Effects on Erbium-Doped Optical Fibers,” *IEEE Trans. Nucl. Sci.* 54 (6), 2426-2434 (2007).
43. Morita, Y., and Kawakami, W., “Dose Rate Effect on Radiation Induced Attenuation of Pure Silica Core Optical Fibers,” *IEEE Trans. Nucl. Sci.* 36 (1), 584-592 (1989).R. L. Farrow, D. A. V. Kliner, P. Schrader, A. A. Hoops, S. W. Moore, G. R. Hadley, R. L. Schmitt, “High-Peak-Power ( $>1.2$  MW) Pulsed Fiber Amplifier,” *Proc. SPIE* 6102, 61020L (2006).